Food Research International 175 (2024) 113687

Contents lists available at ScienceDirect

Food Research International

journal homepage: www.elsevier.com/locate/foodres

Effects of the antimicrobial glabridin on membrane integrity and stress response activation in *Listeria monocytogenes*

Alberto Bombelli [a,b], Carla Araya-Cloutier [b], Sjef Boeren [c], Jean-Paul Vincken [b], Tjakko Abee [a], Heidy M.W. den Besten [a,*]

[a] Food Microbiology, Wageningen University & Research, Wageningen, the Netherlands
[b] Food Chemistry, Wageningen University & Research, Wageningen, the Netherlands
[c] Laboratory of Biochemistry, Wageningen University & Research, Wageningen, the Netherlands

ARTICLE INFO

Keywords:
Natural antimicrobials
Prenylated isoflavonoids
Two-component system
LiaSR
VirRS
Cell envelope
SigmaB regulon
Cross-protection
Mode of action

ABSTRACT

Glabridin is a prenylated isoflavan which can be extracted from liquorice roots and has shown antimicrobial activity against foodborne pathogens and spoilage microorganisms. However, its application may be hindered due to limited information about its mode of action. In this study, we aimed to investigate the mode of action of glabridin using a combined phenotypic and proteomic approach on *Listeria monocytogenes*. Fluorescence and transmission electron microscopy of cells exposed to glabridin showed membrane permeabilization upon treatment with lethal concentrations of glabridin. Comparative proteomics analysis of control cells and cells exposed to sub-lethal concentrations of glabridin showed upregulation of proteins related to the two-component systems LiaSR and VirRS, confirming cell envelope damage during glabridin treatment. Additional upregulation of SigmaB regulon members signified activation of the general stress response in *L. monocytogenes* during this treatment. In line with the observed upregulation of cell envelope and general stress response proteins, sub-lethal treatment of glabridin induced (cross)protection against lethal heat and low pH stress and against antimicrobials such as nisin and glabridin itself. Overall, this study sheds light on the mode of action of glabridin and activation of the main stress responses to this antimicrobial isoflavan and highlights possible implications of its use as a naturally derived antimicrobial compound.

1. Introduction

Listeria monocytogenes is a robust and adaptable foodborne pathogen that can cause listeriosis. Listeriosis is characterized by a low prevalence and high case fatality rate and mainly affects immunocompromised people, the elderly, pregnant women and infants. *L. monocytogenes* is ubiquitous in the environment and can resist different stresses encountered in food and food processing environments (Bucur et al., 2018; Gandhi & Chikindas, 2007). Moreover, it can grow in a wide range of temperatures, pHs and salt concentrations and persist in the food chain (NicAogain & O'Byrne, 2016). Due to these characteristics, *L. monocytogenes* can be present in various raw and processed foods such as deli meat, cold-smoked salmon, cheese and fresh-cut fruit and vegetables, representing an important food safety concern (EFSA and ECDC (European Food Safety Authority and European Centre for Disease Prevention and Control), 2022; Forauer et al., 2021; Zhang et al., 2020).

Natural plant antimicrobials are promising alternatives to inhibit the growth of pathogenic microorganisms and may substitute synthetic preservatives currently used in food and the food industry. Among the variety of plant bioactive compounds, prenylated flavonoids and isoflavonoids (collectively called (iso)flavonoids) showed high antimicrobial activity against foodborne pathogens (Araya-Cloutier et al., 2018a; Ng et al., 2019). Glabridin (Fig. 1) is a monoprenylated isoflavan with antimicrobial activity against foodborne pathogens. It can be extracted from liquorice roots which have been reported to contain 0.24 ± 0.02 mg per g dry roots (van Dinteren et al., 2022). Previous research showed that glabridin had good *in vitro* antimicrobial activity against Gram-positive bacteria such as *Staphylococcus aureus* and *Bacillus subtilis* with a minimum inhibitory concentration (MIC) ranging from 8 to 15 μg/mL (Araya-Cloutier et al., 2018a; Bombelli et al., 2023; Kalli et al., 2021; Lin et al., 2022). Moreover, glabridin has been reported to have anti-biofilm properties when tested against *S. aureus* (Gangwar et al., 2020; Tsukatani et al., 2022). Our previous research showed that glabridin inhibited *L. monocytogenes* at different environmental conditions (MIC 3.1–12.5

* Corresponding author.
E-mail address: heidy.denbesten@wur.nl (H.M.W. den Besten).

https://doi.org/10.1016/j.foodres.2023.113687
Received 28 August 2023; Received in revised form 2 November 2023; Accepted 6 November 2023
Available online 13 November 2023

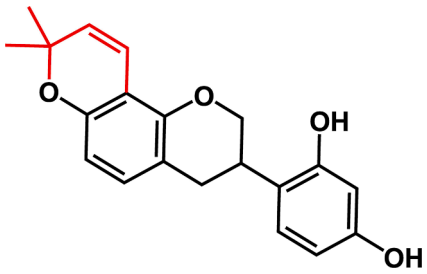

Fig. 1. Structure of the prenylated isoflavan glabridin. The prenyl group is highlighted in red. (For interpretation of the references to colour in this figure legend, the reader is referred to the web version of this article.)

μg/mL) *in vitro* using a microbroth dilution assay and delayed the growth of *L. monocytogenes* in fresh-cut cantaloupe (Bombelli et al., 2023). All these characteristics make glabridin and natural extracts rich in this prenylated isoflavan promising candidates as natural alternatives to synthetic antimicrobials for the food industry.

Despite its potential, the antimicrobial mode of action of glabridin is not fully understood. In general, it has been shown that the main activity of prenylated (iso)flavonoids is due to interaction with the cytoplasmic membrane and subsequent increased permeabilization or disruption (Araya-Cloutier et al., 2018a; Araya-Cloutier et al., 2018b; Wesolowska et al., 2014). For example, morusin, a prenylated flavone, was shown to disrupt the integrity of the cytoplasmic membrane of *S. aureus* by transmission electron microscopy (Pang et al., 2019). Although membrane permeabilization may be the primary effect of glabridin as an antimicrobial agent, other modes of action have also been reported. Previous studies indicated that the antibacterial activity of glabridin against *S. aureus* was caused by the generation of reactive oxygen species (ROS) (Singh et al., 2015) and inhibition of the DNA gyrase (Lin et al., 2022). Therefore, further studies are needed to elucidate the mode of action of glabridin against *L. monocytogenes*.

Proteomic analysis can be used to investigate the mode of action of novel antimicrobial compounds (Schäfer & Wenzel, 2020; Yang et al., 2021). Although proteomics of *S. aureus* treated with glabridin was previously performed, the study focused on the change of surface proteins during biofilm formation (48 h) rather than the antimicrobial mode of action (Gangwar et al., 2020). Short term exposure to glabridin can be used to investigate the mode of action and identify specific stress responses of the cells when subjected to glabridin. In *L. monocytogenes*, various stress mechanisms have been reported; among them, a major component is the activation of SigmaB (SigB), which controls the general stress response (Guerreiro et al., 2020). Previous studies already reported the involvement of the general stress response when *L. monocytogenes* was subjected to antimicrobial compounds such as ampicillin, penicillin and bacteriocins (Begley et al., 2006). Moreover, two-component systems (TCSs) coordinate the response mechanisms to environmental changes, with LiaSR and VirSR being TCSs with an essential role in the cell envelope stress response (Collins et al., 2012; Fritsch et al., 2011; Jiang et al., 2019). The activation of the stress response in *L. monocytogenes* may also induce protection towards different or equal subsequent stresses, thus defined as (cross)protection. (Cross)protection after sub-lethal stresses has already been well reported in *L. monocytogenes*, for example, an increase in nisin resistance after exposure to salt stress (Bergholz et al., 2013) and heat and acid resistance after adaptation to resveratrol (Oliveira et al., 2017). However, to our knowledge, no study has evaluated the stress response of *L. monocytogenes* after exposure to glabridin and the possibility of (cross) protection after exposure to a sub-lethal concentration.

This study aims to investigate the antimicrobial mechanism of glabridin against *L. monocytogenes*. We investigated the effect of glabridin on the permeabilization of the cytoplasmic membrane with fluorescence and transmission electron microscopy. Notably, proteomic analysis was used for the first time to study differences in the proteomic profile of *L. monocytogenes* when exposed to a sub-lethal concentration of glabridin. This analysis allowed us to explore the mode of action of glabridin and characterize the stress response of *L. monocytogenes*. Furthermore, we assessed the possible (cross)protection to stresses after exposure to the sub-lethal stress of glabridin.

2. Materials and methods

2.1. Chemicals and media

Glabridin (purity ≥ 99 %) was purchased from Fujifilm Wako Pure Chemical corporation (Osaka, Japan) and dissolved in dimethyl sulfoxide (DMSO, Merck KGaA, Darmstadt, Germany) to obtain a stock solution (max 40 mg/mL) which was stored at − 20 °C. Tryptone Soya Broth (TSB) and agar bacteriological were purchased from Oxoid Ltd (Basingstoke, UK). Brain Heart Infusion (BHI) was purchased from Becton Dickinson (Le Pont- de- Claix, France). Tris buffer was prepared with 100 mM of Tris (Invitrogen, Aukland, New Zealand) and adjusted to pH 8. Peptone physiological salt solution (PPS) was prepared with 0.1 % (w/v) neutralized bacteriological peptone (Oxoid Ltd) and 0.85 % (w/v) of sodium chloride (Sigma- Aldrich) dissolved in demineralized water. Nisin (from *Lactococcus lactis*, 2.5 % nisin) was purchased from Sigma-Aldrich, and the working solution (0.5 mg/ml) was freshly prepared in 0.02 N HCl and directly used.

2.2. Bacterial strain, culture condition and glabridin treatment

All experiments were carried out with the model strain *L. monocytogenes* EGDe, for which the proteome is the reference in the Uniprot databank (The Uniprot Consortium, 2022). Cells were streaked from − 80 °C glycerol stock on a BHI agar plate and incubated for 24 h at 37 °C. One colony was transferred to 10 mL of TSB and incubated for 18 h at 30 °C in a shaking incubator at 160 revolutions per minute (rpm) to obtain an overnight culture (ON). The ON was then used to inoculate (1:1,000 v/v) 4 mL fresh TSB in polystyrene tubes. The tubes were incubated at 30 °C in a shaking incubator at 160 rpm. After 6 h (OD_{600} = 0.3), glabridin was added at a concentration of 6.25, 12.5 or 25 μg/mL, and tubes were placed back in the incubator at the same condition. Solvent controls were prepared by adding DMSO to a final concentration of 0.06 % (v/v), the maximum concentration reached. The growth of treated and untreated cells was measured by plating appropriate dilutions on BHI plates and checking the optical density at 600 nm (OD_{600}). BHI plates were incubated at 37 °C for 48 h. After 1 h and 2 h of treatment, 100 μL of suspension were stained with SYTO 9 and propidium iodide (PI) at final concentrations of 10 μM and 60 μM, respectively, following the manufacturer's instructions (LIVE/DEAD BacLight Bacterial Viability Kit, ThermoFisher, Eugene, OR, USA). Stained cells were visualized using a Zeiss Axioskop fluorescence microscope. The growth of treated and untreated cells was tested with three independent biological replicates, and each replicate was performed in duplicate.

2.3. Transmission electron microscopy (TEM)

For TEM images, *L. monocytogenes* was cultured as described in section 2.2. Cells were treated with glabridin at a concentration of 25 μg/mL. Solvent controls were prepared by adding DMSO to a final concentration of 0.06 % (v/v). Before and after two hours of treatment, samples were pelleted at 13,800 x *g* for 5 min and fixated in 1 mL of 2.5 % glutaraldehyde in 0.1 M phosphate buffer overnight at 4 °C. Fixed cells were washed twice with 0.1 M phosphate buffer and resuspended in 100 μL of 4 % gelatin in 0.1 M phosphate buffer. Gelatin was solidified at 4 °C, and the specimen was cut into pieces of approximately 3 mm^3. The cubes were fixated in 2.5 % glutaraldehyde for one hour and post-fixated in 1 % osmium tetroxide in 0.1 M phosphate buffer for one hour. Specimens were dehydrated with increasing concentrations of ethanol

(30 %, 50 %, 70 %, 80 %, 90 %, 96 % and twice 100 %) and infiltrated with increasing concentrations of resin in ethanol (33 %, 50 %, 66 % and 100 %). After storing overnight the specimen in 100 % of resin, the resin was polymerized at 70 °C for 8 h. Sections of 50 nm were obtained with a Leica EM UC7 microtome (Leica Microsystems B.V., The Netherlands) and stained with uranyl acetate and lead citrate. Sections were visualized with a JEOL JEM-1400 plus electron microscope (JEOL USA Inc., USA) at 120 kV.

2.4. Proteomics

L. monocytogenes was cultured as described in section 2.2. For the proteome analysis, glabridin was added at a concentration of 6.25 μg/mL, as shown to be the lowest concentration that inhibits the growth of *L. monocytogenes* in the tested condition. Before and after 15 min, 30 min, 1 h and 2 h of glabridin treatment, 4 mL of samples were pelleted at 13,800*g* for 1 min and washed twice with 100 mM Tris buffer (pH 8). The pellet was resuspended in 50 μL of Tris buffer and then stored at −80 °C until further use. Samples treated for 1 h with DMSO (0.06 % v/v) were prepared to verify the effect of the solvent. For each condition, three independent biological replicates were collected and further analyzed.

On the day of proteomic sample preparation, samples were thawed, and cells were lysed by sonication with three cycles of 15 s on ice (Soniprep 150, MSE, London, UK). Proteins were precipitated by adding 200 μL of acetone and incubating the samples for 30 min at room temperature. Afterwards, samples were centrifuged at 13,800*g* for 1 min, the supernatant was removed, and the pellet was resuspended in 100 mM Tris buffer (pH 8). Proteins were quantified with Pierce™ BCA Protein Assay Kit (Thermo Fisher Scientific, USA), and the amount of protein in all samples was standardized to 100 μg of protein in 80 μL of Tris buffer. Samples were prepared according to the filter-aided sample preparation (FASP) (Wisniewski et al., 2009). Briefly, proteins were reduced with 15 mM dithiothreitol, alkylated with 20 mM acrylamide, and digested with trypsin overnight. Each prepared peptide was analyzed by injecting 5 μL into a nanoscale liquid chromatography-tandem mass spectrometry (nanoLC-MS/MS) system (Thermo nLC1000 instrument connected to a Thermo Exploris 480), as described previously (Feng et al., 2022). LC-MS data with all MS/MS spectra were processed with the MaxQuant 2.0.3.0 quantitative proteomics software package (Cox & Mann, 2008), as described previously (Liu et al., 2022). The *L. monocytogenes* EGDe protein database used in the Maxquant analysis was downloaded from UniProt (UniProt identifier UP000000817). Statistical analyses of the MaxQuant ProteinGroups file were performed with Perseus (Tyanova et al., 2016). Reverse hits and contaminants were filtered out. Protein groups were filtered to contain minimally two peptides for protein identification, of which at least one is unique and at least one is unmodified. Proteins were identified as significantly up- or downregulated if the $\log_2$ transformed ratio of the normalized label-free quantitation intensity in the treated samples over the control (before treatment) was above 1 or below −1 with a Benjamini-Hochberg corrected *p*-value smaller than 0.05. Data visualization was performed using R (R Core Team, 2020). The mass spectrometry proteomics data have been deposited to the ProteomeXchange Consortium via the PRIDE (Vizcaíno et al., 2016) partner repository with the dataset identifier PXD043864. The list of proteins regulated by TCSs was based on Fritsch et al. (2011) and Mandin et al. (2005) for LiaSR and VirRS regulated proteins, respectively. SigB regulon was based on Abram et al. (2008); Chatterjee et al. (2006); Guariglia-Oropeza et al. (2018); Hain et al. (2008); Kazmierczak et al. (2003); Liu et al. (2017); Mattila et al. (2020); Oliver et al. (2010); Ollinger et al. (2009); Ryan et al. (2009); Toledo-Arana et al. (2009); Wemekamp-Kamphuis et al. (2004).

2.5. (Cross)protection

To evaluate possible cross-protection towards other stresses after the exposure to sub-lethal concentration of glabridin, untreated or treated cells were further subjected to i) heat inactivation (55 °C), ii) acidic inactivation (pH 3) and iii) nisin treatment (5 μg/mL). Moreover, possible protection toward a subsequential lethal concentration of glabridin was evaluated by subjecting untreated or treated cells to a lethal concentration of glabridin (50 μg/mL). Cells were prepared as described in section 2.2. Before and after 1 h of treatment (glabridin 6.25 μg/mL or DMSO 0.06 % v/v), the cultures were pelleted at 13,800*g* for 1 min and then washed with PPS. Afterwards, the culture was used to inoculate 40 mL of fresh TSB in a glass flask for the heat, acid and nisin inactivation step. For heat inactivation, TSB was preheated and maintained at 55 °C by placing the flask in a water bath. TSB was adjusted to pH 3 with 5 M HCl for the acid inactivation and to a final concentration of nisin of 5 μg/mL for the nisin treatment, and the temperature was maintained constant at 30 °C. For glabridin inactivation, the final volume of TSB with 50 μg/mL of glabridin was 1 mL, and the tube was placed in a thermoblock at 30 °C. The initial inoculum in all treatments was 7.2 ± 0.2 Log CFU/mL. The reduction of treated and untreated cells was measured by plating appropriate dilutions on BHI plates, and the plates were incubated at 37 °C for at least 3 days to allow the recovery of damaged cells. Each condition was tested with three independent biological replicates, and each replicate was performed in duplicate.

3. Results

3.1. Effect of glabridin treatment on growth and propidium iodide (PI) uptake

Glabridin was added at the late exponential phase (6 h) with concentrations ranging from 6.25 μg/mL to 25 μg/mL to verify the effect of the concentration on cell viability and identify the suitable concentration for proteomic analysis. As shown in Fig. 2**A**, glabridin immediately inhibited the growth of *L. monocytogenes* at concentrations equal to 6.25 μg/mL based on cell viability. No difference was measured with 12.5 μg/mL of glabridin compared to 6.25 μg/mL. However, the presence of 25 μg/mL of glabridin decreased the viable count from 8.5 ± 0.1 Log CFU/mL to 5.2 ± 0.7 Log CFU/mL after 2 h of treatment. During the treatment, cells were stained with PI and SYTO9 and visualized with fluorescence microscopy to investigate membrane permeabilization. Fig. 2**B** shows that glabridin induces PI uptake in *L. monocytogenes* depending on the concentration used. Cells treated with 6.25 and 12.5 μg/mL of glabridin showed limited uptake of PI indicating limited permeabilization of the cell with these concentrations (Fig. 2**B**). In line with the viable count, treatment with 25 μg/mL of glabridin resulted in a substantial uptake of PI, indicating that membrane permeabilization occurred during the treatment (Fig. 2**B**). Addition of DMSO (0.06 %) was used as a control, and showed no effect on growth and membrane permeabilization (**Fig. S1**).

3.2. Transmission electron microscopy

TEM of ultrathin sections was used to investigate morphological changes in *L. monocytogenes* after treatment with 25 μg/mL of glabridin. Cells were harvested before or after two hours of glabridin treatment, and representative images are shown in Fig. 3. Untreated cells appeared to have an intact cell envelope, and no defects in the morphology were visualized (Fig. 3**A**). Glabridin induced disruption of the cell envelope and release of intracellular materials (Fig. 3**B-C**, red arrows). Moreover, glabridin treatment resulted in the detachment of the cytoplasmic membrane from the cell wall (Fig. 3**C,** yellow arrows). No visible difference in the cell envelope was detected between untreated and DMSO treated cells (**Fig. S2**).

3.3. Proteomic analysis of glabridin-treated cells

Proteomic analysis was used to study the differences in the proteomic

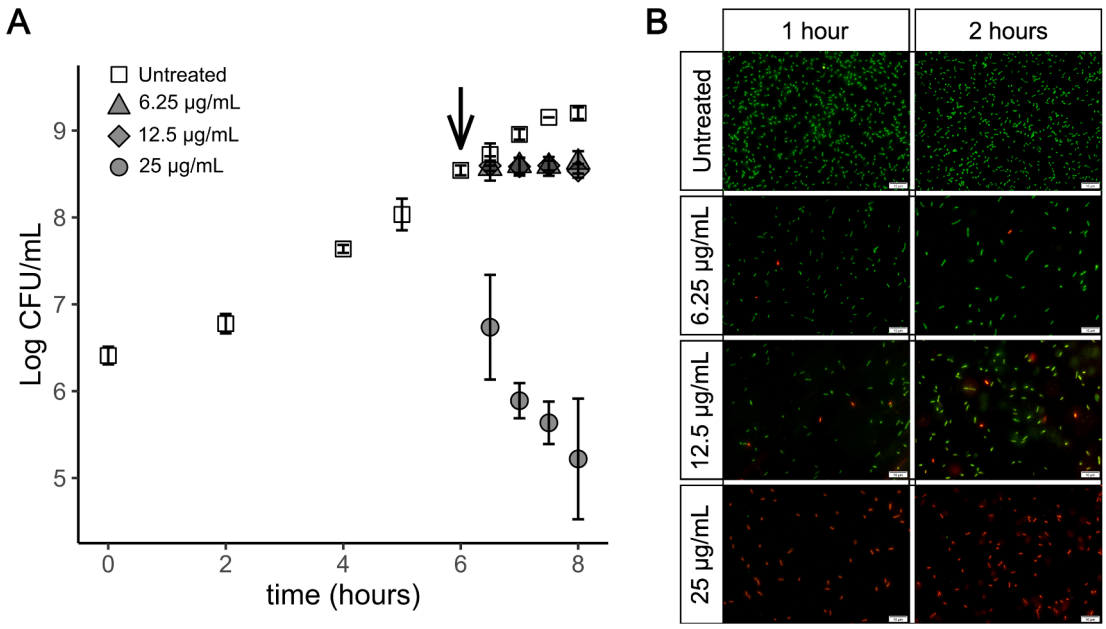

Fig. 2. Growth of *L. monocytogenes* in the presence and absence of glabridin. **A**) Growth curves of untreated cells (empty squares) and glabridin treated cells (filled markers). Cells treated with glabridin are represented with triangles, diamonds and circles for concentrations of 6.25 µg/mL, 12.5 µg/mL and 25 µg/mL, respectively. The arrow represents when the treatment time started. Data are expressed as averages, and error bars represent standard deviations of biologically independent replicates ($n = 3$). **B**) Corresponding fluorescence pictures of samples treated with glabridin or untreated samples. Cells were stained with SYTO9 and PI. Scale bar: 10 µm. (For interpretation of the references to colour in this figure legend, the reader is referred to the web version of this article.)

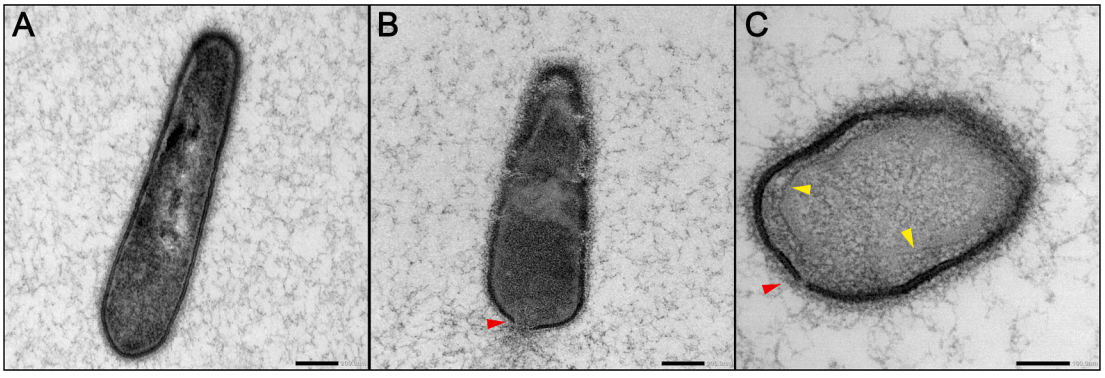

Fig. 3. TEM images of *L. monocytogenes* treated with 25 µg/mL of glabridin. **A**) *L. monocytogenes* untreated cells. **B** and **C**) *L. monocytogenes* treated with 25 µg/mL of glabridin for two hours. Cells were imaged under various angles. Cell envelope damage and detachment of the cell membrane from the cell wall are represented with red and yellow arrows, respectively. The scale bar is 200 nm for **A** and **B** and 100 nm for **C**. (For interpretation of the references to colour in this figure legend, the reader is referred to the web version of this article.)

profile of *L. monocytogenes* before and after sub-lethal glabridin treatment. After reaching the late exponential phase, cells were treated with 6.25 µg/mL of glabridin, and samples were taken before and after 15 min, 30 min, 1 h and 2 h in triplicate. In total, 1,735 proteins were identified and quantified (**Table S1**). The heat map in Fig. 4**A** shows a good separation between treated and untreated samples based on the z-score of label-free quantitation values of the detected proteins. Moreover, samples treated for one and two hours clustered together, showing good separation between treatment times. Fig. 4**B** shows a gradual increase of differently expressed proteins as the treatment length increases, reaching a maximum of 145 upregulated (green) and 196 downregulated (purple) proteins after two hours of treatment. Venn diagrams were used to visualize the number of unique and shared up- and downregulated proteins among the treated samples at different time points (Fig. 4**C and D**). Notably, 34 proteins (19 %, Fig. 4**C**) were upregulated in all time points. As these shared proteins were upregulated immediately after 15 min of treatment, we identified this as the overlap in primary stress response from the cell in the presence of glabridin. Most downregulated proteins (126 proteins, 53 %, Fig. 4**D**) were unique in the sample treated for 2 h, and only four downregulated proteins were shared between the treatment time points (RsbS, lmo0694, lmo2482 and lmo1090, **Table S1**).

The 34 proteins upregulated in all time points were visualized with STRING in Fig. 5. Among the shared upregulated proteins, six proteins (lmo0047, lmo1966, lmo2486-2487 and LiaI - LiaH) are regulated by the TCS LiaSR (highlighted in red**)** and four proteins (AnrA-AnrB, lmo2156 and lmo2439) by another TCS, VirRS (highlighted in blue) (Fritsch et al., 2011; Mandin et al., 2005). Moreover, 13 proteins among the 34 shared upregulated proteins are regulated by SigB (highlighted in black, Fig. 5) (Hain et al., 2008; Kazmierczak et al., 2003; Liu et al., 2017; Ollinger et al., 2009; Ryan et al., 2009). This group includes proteins involved in glycerol metabolism (DhaK-DhaL-DhaM and GlpD) and arginine metabolism (ArgR and ArcA). Finally, proteins related to a general stress response but not regulated by SigB (lmo2830 (thioredoxin), lmo0229,

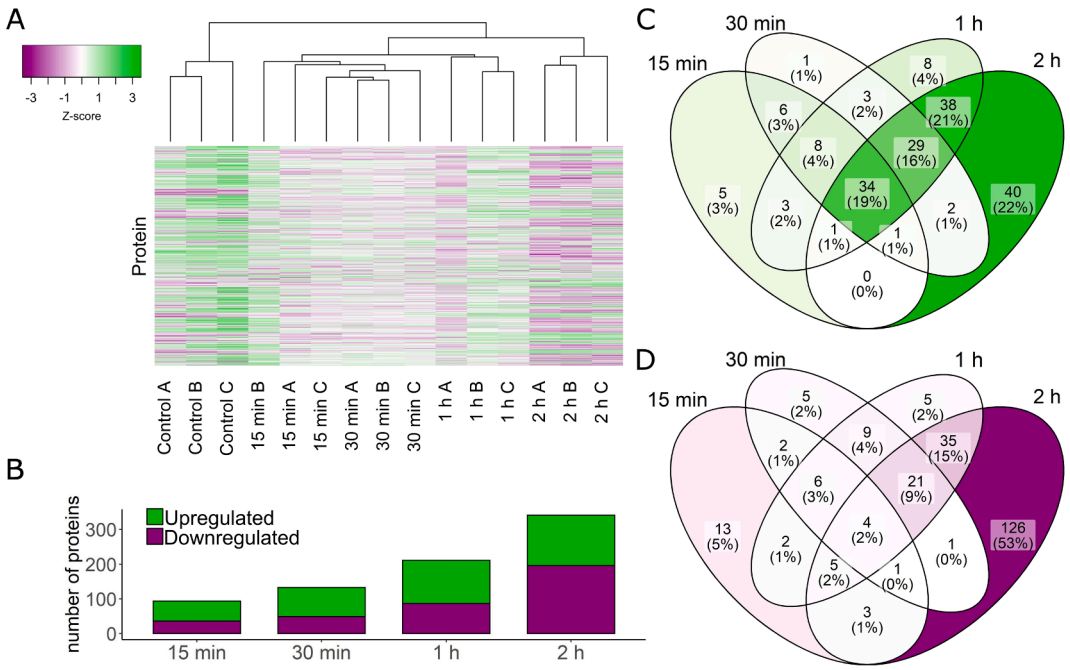

Fig. 4. Differentially expressed proteins of *L. monocytogenes* treated with glabridin (6.25 μg/mL) versus control. **A**) Heat-map represents the clustering of the replicates based on the label free quantitation values of the detected proteins **B**) Number of upregulated (green) and downregulated (purple) proteins compared to control in samples treated with glabridin for 15 min, 30 min, 1 h and 2 h. **C** and **D**) Venn diagrams showing the number of shared and unique upregulated (**C**) and downregulated (**D**) proteins in samples treated with glabridin for different time points. The intensity of the colour is relative to the percentage of proteins in the corresponding area. (For interpretation of the references to colour in this figure legend, the reader is referred to the web version of this article.)

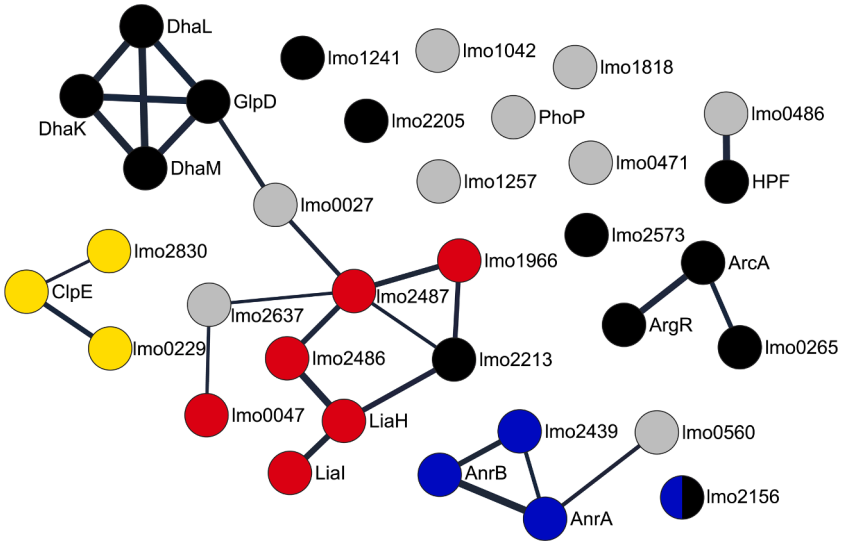

Fig. 5. Protein-protein association predicted using STRING of the shared upregulated protein between samples treated with glabridin (6.25 μg/mL) after 15 min, 30 min, 1 h and 2 h. Dots represent all the shared upregulated proteins. Thicker lines represent stronger associations. Different colour highlights proteins regulated by the two component systems (LiaSR and VirRS, in red and blue, respectively), SigB regulated proteins (in black), stress response proteins (in yellow) and others (grey). Lmo2156 has been reported to be regulated by both VirRS and SigB. (For interpretation of the references to colour in this figure legend, the reader is referred to the web version of this article.)

ClpE) were shown to be upregulated in all time points (highlighted in yellow).

Fig. 6 shows a volcano plot of differentially expressed proteins in the glabridin-treated sample for two hours compared to untreated cells, highlighting proteins regulated by the TSCs LiaSR and VirRS, and SigB. These proteins represented 44.1 % of the upregulated proteins and covered the area of most significant proteins, indicating a remarkable activation of the LiaSR, VirRS, and SigB dependent stress responses in the presence of sublethal concentrations of glabridin.

Table 1 shows the list of differently expressed proteins in at least one time point regulated by LiaSR and VirRS. Overall, the expression of proteins regulated by LiaSR increased during the treatment. For example, LiaI and LiaH were upregulated immediately after 15 min of exposure, and after two hours, the fold change reached 16.0 and 26.6 for LiaI and LiaH, respectively. LiaI is a membrane protein that binds the phage shock protein (Psp) homologue LiaH. LiaS and LiaF (the histidine kinase and a protein which controls the activity of LiaS, respectively) were similarly upregulated after 30 min of treatment compared to

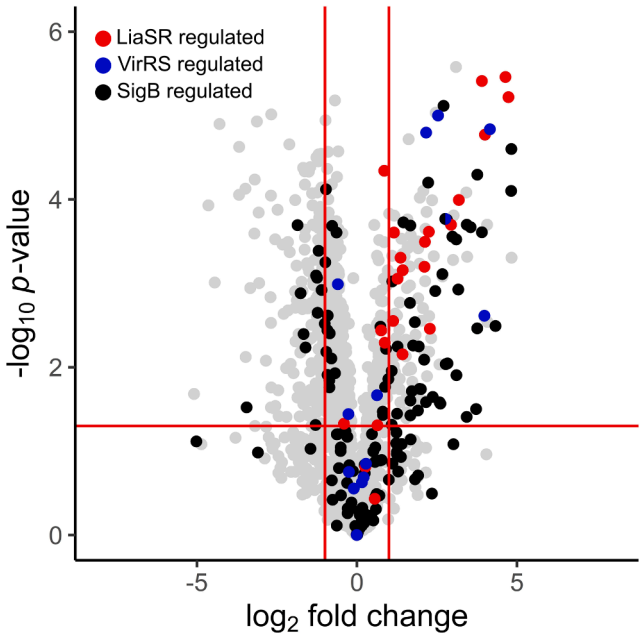

Fig. 6. Volcano plot of proteins expressed in *L. monocytogenes* treated with glabridin (6.25 μg/mL) for two hours compared to untreated control. Dots represent all the detected proteins. Different colours highlight protein regulated by the two component systems (LiaSR and VirRS, in red and blue, respectively), SigB regulated proteins (in black) and others (grey). Lmo2156 has been reported to be regulated by both VirRS and SigB. Red lines represent the cut off values used for the definition of different regulated proteins (p-value < 0.05, log2 fold change > 1 or < -1). (For interpretation of the references to colour in this figure legend, the reader is referred to the web version of this article.)

untreated cells reaching 2.7 fold change after two hours of treatment. Lmo2486-2487 are part of the same operon and were shown to be strongly upregulated in the treated samples; lmo2487 is a homologue of YvlB of *B. subtilis,* which is part of the Psp response network (Nielsen et al., 2012; Popp et al., 2022). Lmo1966 and lmo1967 (*telA*) form an operon and were upregulated, reaching a 9.1 and 4.7-fold change, respectively, compared to the control after two hours of treatment. TelA is a mediator of resistance to a number of cell envelope-acting antimicrobials (Collins et al., 2010b). Moreover, ABC transporters regulated by LiaSR, such as lmo0194-0195, lmo1636 and lmo2745, were upregulated compared to untreated samples, with fold changes ranging from 2.2 to 4.3 after 2 h of exposure. None of the proteins regulated by LiaSR were differently expressed in the DMSO control samples (**Table S2**), indicating that this stress response is specific to the glabridin treatment.

Among the proteins regulated by VirRS, AnrA and AnrB form an ABC transporter that was immediately upregulated. AnrA and AnrB were upregulated with increasing values as the treatment length increased, reaching a 4.5 and 5.8 fold change after two hours, respectively. Moreover, the two hypothetical proteins lmo2156 and lmo2439 were more expressed in all time points than the control. Although the D-alanyl carrier protein (DCP) involved in the D-alanylation of lipoteichoic acid was upregulated after 1 h of treatment, a similar fold change was observed in the DMSO control sample (Table S2). Overall, the upregulation of proteins controlled by the TCSs LiaSR and VirRS indicated that glabridin induced the activation of the cell-envelope stress response, including upregulation of the Psp and ABC transporters.

Table 2 shows the proteins regulated by SigB that were upregulated in at least one time point during two hours of treatment, indicating a general stress response from *L. monocytogenes* in the presence of glabridin. For example, the general stress protein Ctc and the universal stress protein (lmo0515) were upregulated with a fold change ranging from 13.6 to 28.2 after 2 h of exposure. Proteins associated with general stress response, such as lmo1580 and lmo1601, were also upregulated in the treated samples. Proteins with protease and peptidase activity were also upregulated, such as ClpC, ClpP and htrA, which are known to cleave misfolded proteins formed during various environmental stresses (Abfalter et al., 2019; Illigmann et al., 2021). The upregulation of oxidoreductase-related proteins, such as superoxide dismutase and heme-degrading monooxygenase, points to oxidative stress upon

Table 1
Differently regulated proteins in *L. monocytogenes* cells treated with 6.25 μg/mL of glabridin whose expression is controlled by TCSs LiaSR and VirRS. Fold change compared to untreated cells was measured after 15 min, 30 min, 1 h and 2 h of exposure. Protein name and function are obtained from KEGG and Uniprot if not differently stated.

Gene name	Protein	15 min	30 min	1 h	2 h
LiaSR regulated protein					
lmo0954-liaI	LiaI *	3.1	4.4	8.8	16.0
lmo0955-liaH	LiaH *	4.3	7.6	16.4	26.6
lmo1020-liaF	LiaF *	n.s.	1.4	2.1	2.7
lmo1021-liaS	LiaS * - two-component sensor histidine kinase	n.s.	1.4	2.2	2.7
lmo2486	hypothetical protein	3.6	6.2	12.4	15.0
lmo2487	hypothetical protein, *B. subtilis* YvlB homologue	5.0	7.9	16.5	25.0
lmo1966	hypothetical protein	2.6	3.4	6.0	9.1
lmo1967-telA §	hypothetical protein	n.s.	2.0	3.3	4.7
lmo0193	hypothetical protein	n.s.	n.s.	1.6	2.6
lmo0194	ABC transporter, ATP-binding protein	n.s.	n.s.	2.0	2.4
lmo0195	ABC transporter, permease	n.s.	n.s.	1.5	2.2
lmo1636	ABC transporter, ATP-binding protein	1.3	1.5	1.8	2.2
lmo2745	ATP-binding/permease protein	1.7	2.3	3.6	4.3
lmo0047	hypothetical protein	2.6	3.0	4.0	4.4
lmo2258	hypothetical protein	2.9	3.8	n.s.	7.7
lmo2224	hypothetical protein	n.s.	n.s.	3.0	4.9
VirRS regulated protein					
lmo2114	AnrA †- ABC transporter ATP-binding protein	2.9	3.7	4.5	4.5
lmo2115	AnrB †- ABC transporter permease	3.1	4.7	5.7	5.8
lmo2156	hypothetical protein	5.7	6.0	7.5	6.8
lmo2439	hypothetical protein	12.9	16.7	17.3	17.8
lmo0972-dltC	D-alanyl carrier protein (DCP)	n.s.	n.s.	8.9	15.8

* according to Fritsch et al. (2011)
§ according to Collins et al. (2010b)
† according to Collins et al. (2010a)
n.s.: not significant

Table 2
Upregulated proteins in *L. monocytogenes* cells treated with 6.25 μg/mL of glabridin whose expression is controlled by SigB. Fold change compared to untreated cells was measured after 15 min, 30 min, 1 h and 2 h of exposure. Protein name and function are obtained from KEGG and Uniprot if not differently stated.

Gene name	Protein	15 min	30 min	1 h	2 h
General stress response					
lmo0211-ctc	General stress protein Ctc	1.9	3.5	8.0	13.6
lmo0231-mcsB	Protein-arginine kinase	n.s.	2.1	3.6	3.2
lmo0232-clpC	Endopeptidase Clp ATP-binding chain C	n.s.	2.3	4.2	4.7
lmo0292-htrA	Heat-shock protein htrA serine protease	n.s.	2.2	4.8	6.4
lmo0515	Universal stress protein UspA	n.s.	11.7	17.6	28.2
lmo1138-clpP	ATP-dependent Clp protease proteolytic subunit	n.s.	2.8	5.4	6.5
lmo1580	Universal stress protein	1.9	2.7	3.6	3.2
lmo1601	General stress protein	n.s.	n.s.	1.9	2.1
lmo1879-cspD	Cold-shock protein	2.8	n.s.	n.s.	n.s.
lmo2230	Arsenate reductase	n.s.	6.0	n.s.	7.1
lmo2468 -clpP	ATP-dependent Clp protease proteolytic subunit	n.s.	1.6	2.1	2.7
Oxidative stress response					
lmo1439-sodA	Superoxide dismutase	n.s.	1.8	2.0	3.4
lmo2191-spx	Global transcriptional regulator Spx	2.4	2.2	1.7	n.s.
lmo2213	Heme-degrading monooxygenase	4.7	5.7	6.5	6.8
Acid stress response					
lmo0043-arcA	Arginine deiminase ArcA	4.2	4.0	4.0	3.9
lmo0796	Hypothetical protein	n.s.	n.s.	n.s.	4.5
lmo0913	Succinate semialdehyde dehydrogenase	n.s.	n.s.	n.s.	6.0
lmo1367-argR	Arginine repressor ArgR	2.3	3.5	3.7	5.5
lmo2391	Hypothetical protein	n.s.	n.s.	5.9	6.1
lmo2434	Glutamate decarboxylase	n.s.	n.s.	10.4	10.8
Metabolism					
lmo0265	Succinyl-diaminopimelate desuccinylase	13.6	17.2	27.0	28.4
lmo0539-lacD	Tagatose 1,6-diphosphate aldolase	n.s.	n.s.	3.3	4.3
lmo0554	NADH-dependent butanol dehydrogenase	2.0	1.8	2.3	1.8
lmo0783	PTS mannose transporter subunit IIB	n.s.	n.s.	n.s.	3.2
lmo0784	PTS mannose transporter subunit IIB	n.s.	n.s.	2.3	n.s.
lmo0956	N-acetylglucosamine-6P-phosphate deacetylase	n.s.	n.s.	2.0	2.1
lmo1293-glpD	Glycerol-3-phosphate dehydrogenase GlpD	2.7	5.2	7.3	7.9
lmo1538-glpK	Glycerol kinase	n.s.	2.0	2.5	2.4
lmo1830	Short-chain dehydrogenase	n.s.	n.s.	12.7	13.2
lmo2205-gpmA	Phosphoglyceromutase	2.6	3.8	5.1	7.0
lmo2511-hpf	Ribosome hibernation promoting factor (HPF)	2.8	4.4	8.9	11.7
lmo2573	Zinc-binding dehydrogenase	4.6	5.2	6.6	8.6
lmo2695-dhaK	Dihydroxyacetone kinase subunit DhaK	3.9	6.2	10.8	10.8
lmo2696-dhaL	Dihydroxyacetone kinase subunit DhaL	4.7	8.2	13.1	13.5
lmo2697-dhaM	Phosphoenolpyruvate - glycerone phosphotransferase subunit DhaM	3.0	6.0	10.1	9.0
Other/unknown functions					
lmo0134	Hypothetical protein	n.s.	6.3	10.0	8.6
lmo0170	Hypothetical protein	n.s.	2.1	3.1	3.5
lmo0407	Hypothetical protein	n.s.	n.s.	n.s.	20.1
lmo0629	Hypothetical protein	n.s.	n.s.	n.s.	2.1
lmo0654	Hypothetical protein	n.s.	3.1	4.0	4.0
lmo0794	Hypothetical protein	n.s.	4.1	5.8	15.0
lmo1241	Hypothetical protein	3.4	3.8	3.5	3.2
lmo1261	Hypothetical protein	2.7	3.1	3.2	n.s.
lmo1526	Hypothetical protein	n.s.	1.9	1.9	3.3
lmo1694	CDP-abequose synthase	n.s.	n.s.	n.s.	5.2
lmo2156	Hypothetical protein	5.7	6.0	7.5	6.8
lmo2494	Phosphate-specific transport system accessory protein PhoU	n.s.	n.s.	n.s.	2.4
lmo2572	Dihydrofolate reductase subunit A	n.s.	2.3	3.1	3.8
lmo2673	Hypothetical protein	n.s.	3.0	3.1	3.7

n.s.: not significant

exposure to glabridin. Regarding the acid stress response, upregulation of arginine deiminase ArcA (lmo0043) and the arginine repressor ArgR (lmo1367) indicated upregulation of the arginine deiminase (ADI) pathway. Moreover, the upregulation of glutamate decarboxylase (lmo2434) indicated the activation of the glutamate decarboxylase (GAD) pathway. ADI and GAD pathways are involved in acid resistance in *L. monocytogenes* (Karatzas et al., 2012; Ryan et al., 2009). Although ArgR was similarly upregulated in the DMSO control sample (**Table S2**), no upregulation of ADI or GAD pathway proteins was measured in the DMSO control sample. The upregulated proteins part of the SigB regulon also showed changes in the metabolism of *L. monocytogenes*. The most upregulated protein was lmo0265 (28.4 fold change after 2 h), a succinyl-diaminopimelate desuccinylase involved in lysine metabolism. Moreover, the upregulation of proteins involved in glycerol utilization (GlpD, glpK and DhaK-DhaL-DhaM) indicated changes in carbon metabolism.

3.4. (Cross)protection

The increase in expression of the cell envelope and general stress defence protein regulated by LiaSR, VirRS and SigB after sublethal glabridin treatment may provide protection against subsequential other lethal stresses. To test this hypothesis, control cells (no pretreatment) and cells pre-treated with 6.25 μg/mL of glabridin for one hour were subsequentially exposed to a lethal treatment for 20 min. The lethal stresses included heat (55 °C), low pH (3), and high concentrations of nisin and glabridin (5 μg/mL and 50 μg/mL, respectively). Fig. 7 shows the reduction of viable cells after 20 min of treatment compared to the

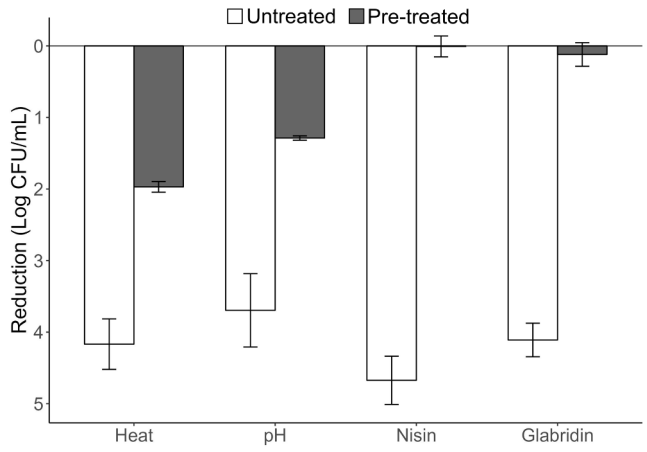

Fig. 7. Reduction of *L. monocytogenes* after 20 min of treatment at 55 °C (heat), pH 3 (pH) and with 5 μg/mL of nisin and 50 μg/mL of glabridin. Reduction of untreated cell is represented by empty bars and reduction of cells treated with 6.25 μg/mL of glabridin for one hour are represented with filled bars. Data are expressed as averages and error bars represent standard deviations of biologically independent replicates ($n = 3$).

initial inoculum. Control cells showed a significantly higher reduction than glabridin pre-treated cells, indicating that pre-exposure to glabridin increased the resistance of *L. monocytogenes* to the tested lethal stresses. Reduction in viable cells for the control cells was similar between the tested stresses, with an average reduction of 4.2 ± 0.5 Log CFU/mL. Cells pre-exposed to glabridin showed a reduction of 2.0 ± 0.1 Log CFU/mL and 1.3 ± 0.0 Log CFU/mL after 20 min of treatment at 55 °C and pH 3, respectively. Notably, no reduction in viable cells of glabridin pre-treated samples was measured after 20 min of treatment with a lethal concentration of nisin and glabridin (5 μg/mL and 50 μg/mL, respectively). No significant difference ($p > 0.05$) was observed between untreated cells and DMSO control (**Fig. S3**), indicating that the (cross)protection against lethal stresses is due to the pretreatment with glabridin.

4. Discussion

This study aimed to explore the mode of action of glabridin, a promising natural antimicrobial compound, against *L. monocytogenes*. The main effects of glabridin against *L. monocytogenes* are summarized in Fig. 8. We showed that *L. monocytogenes* activated the TCSs LiaSR and VirRS, which play a key role in orchestrating the cell envelope stress response in *L. monocytogenes* and other Gram-positive bacteria such as *B. subtilis* (Jordan et al., 2008; Nielsen et al., 2012). Moreover, the upregulation of proteins part of the SigB regulon and other stress-related proteins indicated the activation of the general stress response in *L. monocytogenes*.

4.1. Glabridin treatment permeabilize the cytoplasmic membrane

This study showed that glabridin caused cytoplasmic membrane permeabilization in *L. monocytogenes*. The tested PI uptake upon exposure indicates that glabridin caused interruptions in membranes larger than 1.5 nm based on the PI molecular size (Bowman et al., 2010). Previous studies reported membrane permeabilization and dissipation of proton motive force of *S. aureus* after exposure to glabrol, α-mangostin, isobavachalcone and morusin, all prenylated phenolic compounds (Pang et al., 2019; Song et al., 2021; Wu et al., 2019b). TEM images confirmed that exposure to glabridin resulted in the disruption of the cell envelope and shrinkage of the cytoplasmic membrane of *L. monocytogenes*. In line with the results presented here, previous studies showed that kuwanon G and morusin, both prenylated flavones, induced separation of the cytoplasmic membrane and destruction of the cell envelope in *S. aureus* with TEM imaging (Pang et al., 2019; Wu et al., 2019a). Our previous study indicated that glabridin induced limited permeabilization in *L. monocytogenes*. (Araya-Cloutier et al., 2018a). However, lower concentrations tested and the use of a different method may explain this difference. Overall, this study indicates that the bactericidal activity of glabridin can be explained by membrane permeabilization and cell envelope disruption in *L. monocytogenes*.

4.2. Glabridin induces cell-envelope stress responses via the TCSs LiaSR and VirRS

The TCS LiaSR is known to regulate the expression of 29 genes (Fritsch et al., 2011), and among them, 16 were shown to be upregulated upon exposure to glabridin, indicating activation of this TCS. The TCS LiaSR has been reported to be activated in *L. monocytogenes* when cell envelope-acting antimicrobials are applied, such as nisin and bacitracin (Fritsch et al., 2011; Pinilla et al., 2021). Therefore, the activation of LiaSR after exposure to glabridin supports the hypothesis that glabridin

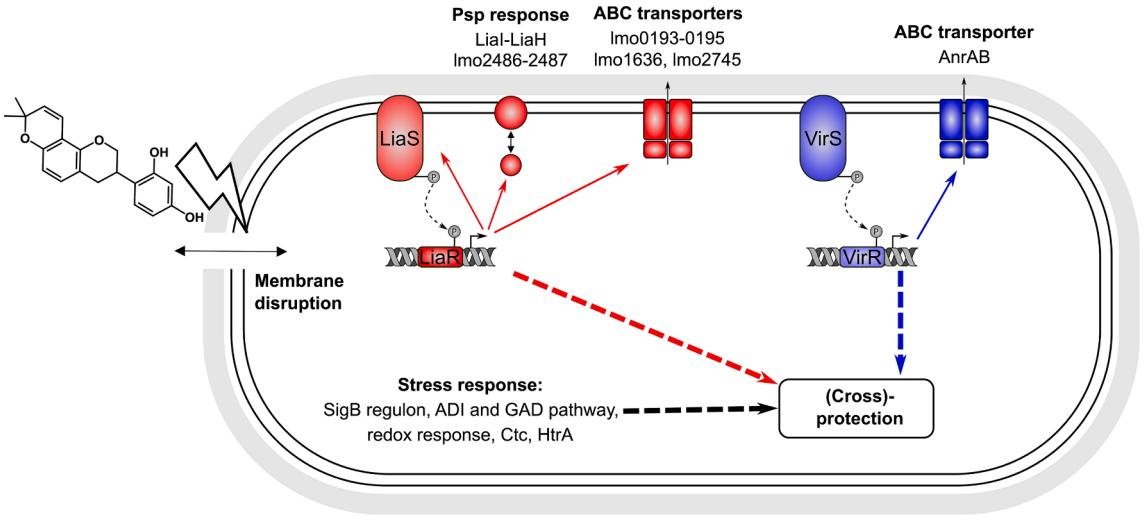

Fig. 8. Overview of main effects of glabridin treatment against *L. monocytogenes*. Different colours highlight the involvement of the two component systems LiaSR and VirRS in red and blue, respectively. Psp: phage shock protein. See text for details. (For interpretation of the references to colour in this figure legend, the reader is referred to the web version of this article.)

is active on the cell envelope of *L. monocytogenes*.

The proteomic profile shows that LiaI and LiaH were part of the main upregulated proteins in response to glabridin. The *liaIH* operon is reported to be the main target of the response regulator LiaR upon activation of the TCS, and it is part of the Psp stress response in *L. monocytogenes* (Domínguez-Escobar et al., 2014). LiaI is a membrane protein that can bind to LiaH, which contains a PspA domain. This complex formation is enhanced during cell envelope stress and may confer protection to the cytoplasmic membrane (Domínguez-Escobar et al., 2014). The Psp stress response is a well-studied cellular response upon cell envelope stress (Flores-Kim & Darwin, 2016; Joly et al., 2010). However, few studies focused on the Psp response in *L. monocytogenes*. In addition to LiaH, the only protein that contains a PspA domain in *L. monocytogenes*, lmo2485 and lmo2486 contain a PspC domain (Popp et al., 2022). Interestingly, lmo2485 and lmo2486 are part of the same operon (lmo2484-2487, (Toledo-Arana et al., 2009)), which is also regulated by LiaSR. Although lmo2485 was not detected in our proteomic experiment, lmo2486 was highly upregulated after exposure to glabridin. Lmo2487 was also highly upregulated in the presence of glabridin and reported to be a homologue of YvlB of *B. subtilis* (Nielsen et al., 2012), which is part of the Psp response network in *B. subtilis* (Popp et al., 2022). The operon lmo2484-2487 has been reported to be upregulated during treatment with cell wall antibiotic cefuroxime (Nielsen et al., 2012), highlighting its importance for cell envelope antimicrobials in *L. monocytogenes*.

Different ABC transporters regulated by the TCSs LiaSR and VirRS were upregulated after exposure to glabridin. The most characterized upregulated ABC transporter was AnrAB. AnrAB was reported to be involved in the detoxification of cell-envelope active antimicrobials such as nisin and bacitracin (Collins et al., 2010a; Jiang et al., 2019; Rismondo & Schulz, 2021), and its upregulation indicates cell-envelope stress in the presence of glabridin. AnrAB is regulated by the TCS VirRS, which has already been reported to have an essential role in *L. monocytogenes* exposed to antimicrobials which affect membrane integrity, such as nisin, lauric arginate, ε-polylysine (Kang et al., 2015; Pang et al., 2022; Pinilla et al., 2021).

Among the upregulated ABC transporters under the control of LiaSR, lmo2745 has high similarity with BmrA of *B. subtilis* (also known as YvcC), the multidrug resistance ABC transporter (Steinfels et al., 2004). BmrA forms a homodimer which has been shown to export toxic compounds in *B. subtilis* (Chami et al., 2002; Rismondo & Schulz, 2021); however, lmo2745 has not been studied in detail in *L. monocytogenes*. The upregulation of lmo1636 and lm0193-0195 shows that other ABC transporters are involved in response to glabridin. Lmo1636 forms an ABC transporter with lmo1637 (upregulated less than two-fold, **Table S1**). Orthologs of these transporters are defined as bacitracin ABC transporter, highlighting the importance of this transporter for cell envelope active antimicrobials. The operon lmo0193-0195 encodes for an ABC transporter formed by lmo0195 and lmo0194 and an additional protein, lmo0193. Interestingly, lmo0195 contains a MacB domain and lmo0193 a HlyD domain, both characteristic of ABC multidrug efflux transporters (Delmar et al., 2014; Greene et al., 2018). Overall, the proteomic profile of *L. monocytogenes* exposed to glabridin indicates the activation of the cell-envelope stress response orchestrated by LiaSR and VirRS, which may be confirmed in follow-up studies by mutation of the selected genes.

4.3. Activation of the general stress response

The increased presence of stress-related proteins, including the ones regulated by SigB, indicated that *L. monocytogenes* responds to glabridin by activating the general stress response. Notably, one of the proteins downregulated in all time points was RsbS, which is part of the stressosome and has a key role in the signal cascade that activates SigB (Guerreiro et al., 2020). Among the SigB regulon, upregulation of the ADI and GAD pathway indicates acidic stress, which may be related to the inability of *L. monocytogenes* to regulate the internal pH due to the permeabilization of the membrane, as previously suggested for other membrane active antimicrobial compounds (Song et al., 2021). Moreover, the upregulation of the general stress protein Ctc and the serine protease HtrA (regulated by SigB) indicates major changes in the proteome of *L. monocytogenes*. Overexpression of the *ctc* gene (lmo0211) and *htrA* gene (lmo0292) was reported in *L. monocytogenes* after exposure to the cefuroxime and the bacteriocin pediocin (Laursen et al., 2015; Nielsen et al., 2012). Induction of the SigB regulon after exposure to cell envelope-acting antimicrobials has also been shown in other Gram-positive bacteria, such as in the response of *B. subtilis* in the presence of bacitracin (Mascher et al., 2003). Sivaranjani et al. (2019) reported the upregulation of general stress response proteins such as Clp, sodA in *Staphylococcus epidermidis* after exposure to α-mangostin, a prenylated xanthone reported to affect membrane integrity in Gram-positive bacteria.

Notably, our comparative proteome analysis of *L. monocytogenes* cells exposed to sublethal concentrations of glabridin provided new insights into this pathogen's primary and secondary response against this membrane active antimicrobial. Previous studies reported that glabridin induced the generation of ROS in *S. aureus* (Singh et al., 2015). In our proteomic data, the upregulation of proteins related to oxidative stress (such as thioredoxin-lmo2830 and superoxide dismutase) indicates that ROS accumulation might occur in *L. monocytogenes* during glabridin treatment. As proteins involved in cell envelope stress described above (**Section 4.2**) and proteins related to oxidative stress were upregulated immediately after 15 min of treatment, both responses may be linked to a primary effect of glabridin on the cell membrane. Possible perturbation of the membrane homeostasis can lead to defects in the respiratory chain which may be the source of ROS. Choi et al. (2015) highlighted this hypothesis for an antimicrobial peptide which caused permeabilization of the cytoplasmic membrane and increased ROS in *E. coli*. Previous studies have also reported the induction of secondary oxidative stress upon exposure to cell envelope-acting antimicrobials, such as nisin, daptomycin and other antimicrobial peptides (Liu et al., 2015; Miyamoto et al., 2015; Po et al., 2021; Schäfer & Wenzel, 2020).

4.4. Sub-lethal treatment with glabridin can induce (cross)-protection

Our data show that exposure to sub-lethal concentrations of glabridin induced (cross)protection against heat, low pH, nisin and glabridin itself. Increased resistance to heat and low pH can be explained by the activation of the general stress response, as previous studies related this phenotype to the upregulation of the SigB regulon (Koomen et al., 2021). Proteins such as Ctc, HtrA and Clp are known to be involved in response to heat stress, whereas the GAD and ADI pathways are part of the acid tolerance response (NicAogain & O'Byrne, 2016; Soni et al., 2011). Their upregulation may explain the induced cross-protection by the pretreatment with glabridin. Notably, the pre-exposure to a sublethal concentration of glabridin, induced higher resistance towards lethal concentrations of nisin and glabridin than other stresses, suggesting similarities between the mode of action of glabridin and nisin and further indicating the cell envelope as the primary target of glabridin. Different mechanisms have been reported to contribute to the resistance of *L. monocytogenes* to nisin, including the activation of VirRS and LiaSR regulon members (Bergholz et al., 2013). Among the proteins regulated by LiaSR, TelA (lmo1967) has been found to contribute to the resistance of *L. monocytogenes* to nisin and bacitracin (Collins et al., 2010a; Collins et al., 2010b). Therefore, activation of these TCSs might explain the higher resistance to nisin treatment. These results highlight possible implications of using glabridin as an antimicrobial compound and the need to evaluate its antimicrobial efficacy if applied with other antimicrobials or as part of hurdle technology. Notably, understanding the stress response of cells in the presence of glabridin can help identify the correct use and support application of this novel antimicrobial in the food industry.

5. Conclusion

In conclusion, this study described the phenotypic and proteomic response of *L. monocytogenes* to (sub)lethal concentrations of glabridin to elucidate the mode of action of this antimicrobial. PI uptake and TEM confirmed permeabilization of the cytoplasmic membrane upon exposure to lethal concentrations of glabridin, suggesting that the mode of action of glabridin relies upon the interaction with bacterial membranes. This was further confirmed in proteomic studies that revealed the activation of a specific cell-envelope damage repair response characterized by the activation of TCSs LiaSR and VirRS. In addition, a Sigma B-dependent general stress defence response was activated by a sub-lethal concentration of glabridin, resulting in (cross)protection towards subsequential selected lethal food-preservation stresses.

CRediT authorship contribution statement

Alberto Bombelli: Conceptualization, Investigation, Formal analysis, Writing – original draft. **Carla Araya-Cloutier:** Conceptualization, Writing – review & editing, Supervision. **Sjef Boeren:** Investigation, Formal analysis, Writing – review & editing. **Jean-Paul Vincken:** Writing – review & editing, Supervision. **Tjakko Abee:** Conceptualization, Writing – review & editing, Supervision. **Heidy M.W. den Besten:** Conceptualization, Writing – review & editing, Supervision.

Declaration of Competing Interest

The authors declare that they have no known competing financial interests or personal relationships that could have appeared to influence the work reported in this paper.

Data availability

Data will be made available on request.

Acknowledgements

The authors would like to thank Jelmer Vroom from the Wageningen Electron Microscopy Centre (WEMC) for his contribution during the TEM imaging and Uyen Phuong Nguyen for assistance with the cross-protection experiment.

Appendix A. Supplementary material

Supplementary data to this article can be found online at https://doi.org/10.1016/j.foodres.2023.113687.

References

Abfalter, C. M., Bernegger, S., Jarzab, M., Posselt, G., Ponnuraj, K., & Wessler, S. (2019). The proteolytic activity of *Listeria monocytogenes* HtrA. *BMC Microbiology, 19*(1), 255. https://doi.org/10.1186/s12866-019-1633-1

Abram, F., Starr, E., Karatzas, K. A., Matlawska-Wasowska, K., Boyd, A., Wiedmann, M., … O'Byrne, C. P. (2008). Identification of components of the sigma B regulon in *Listeria monocytogenes* that contribute to acid and salt tolerance. *Applied and Environmental Microbiology, 74*(22), 6848–6858. https://doi.org/10.1128/aem.00442-08

Araya-Cloutier, C., Vincken, J. P., van de Schans, M. G. M., Hageman, J., Schaftenaar, G., den Besten, H. M. W., & Gruppen, H. (2018a). QSAR-based molecular signatures of prenylated (iso)flavonoids underlying antimicrobial potency against and membrane-disruption in Gram positive and Gram negative bacteria. *Scientific Reports, 8*(1), 9267. https://doi.org/10.1038/s41598-018-27545-4

Araya-Cloutier, C., Vincken, J. P., van Ederen, R., den Besten, H. M. W., & Gruppen, H. (2018b). Rapid membrane permeabilization of *Listeria monocytogenes* and *Escherichia coli* induced by antibacterial prenylated phenolic compounds from legumes. *Food Chemistry, 240*, 147–155. https://doi.org/10.1016/j.foodchem.2017.07.074

Begley, M., Hill, C., & Ross, R. P. (2006). Tolerance of *Listeria monocytogenes* to cell envelope-acting antimicrobial agents is dependent on SigB. *Applied and Environmental Microbiology, 72*(3), 2231–2234. https://doi.org/10.1128/AEM.72.3.2231-2234.2006

Bergholz, T. M., Tang, S., Wiedmann, M., & Boor, K. J. (2013). Nisin resistance of *Listeria monocytogenes* is increased by exposure to salt stress and is mediated via LiaR. *Applied and Environmental Microbiology, 79*(18), 5682–5688. https://doi.org/10.1128/AEM.01797-13

Bombelli, A., Araya-Cloutier, C., Vincken, J.-P., Abee, T., & den Besten, H. M. W. (2023). Impact of food-relevant conditions and food matrix on the efficacy of prenylated isoflavonoids glabridin and 6,8-diprenylgenistein as potential natural preservatives against *Listeria monocytogenes*. *International Journal of Food Microbiology, 390*, Article 110109. https://doi.org/10.1016/j.ijfoodmicro.2023.110109

Bowman, A. M., Nesin, O. M., Pakhomova, O. N., & Pakhomov, A. G. (2010). Analysis of plasma membrane integrity by fluorescent detection of Tl+ uptake. *The Journal of Membrane Biology, 236*(1), 15–26. https://doi.org/10.1007/s00232-010-9269-y

Bucur, F. I., Grigore-Gurgu, L., Crauwels, P., Riedel, C. U., & Nicolau, A. I. (2018). Resistance of *Listeria monocytogenes* to stress conditions encountered in food and food processing environments. *Frontiers in Microbiology, 9*, 2700. https://doi.org/10.3389/fmicb.2018.02700

Chami, M., Steinfels, E., Orelle, C., Jault, J.-M., Di Pietro, A., Rigaud, J.-L., & Marco, S. (2002). Three-dimensional structure by cryo-electron microscopy of YvcC, an homodimeric ATP-binding cassette transporter from *Bacillus subtilis*. *Journal of Molecular Biology, 315*(5), 1075–1085. https://doi.org/10.1006/jmbi.2001.5309

Chatterjee, S. S., Hossain, H., Otten, S., Kuenne, C., Kuchmina, K., Machata, S., … Hain, T. (2006). Intracellular gene expression profile of *Listeria monocytogenes*. *Infection and Immunity, 74*(2), 1323–1338. https://doi.org/10.1128/IAI.74.2.1323-1338.2006

Choi, H., Yang, Z., & Weisshaar, J. C. (2015). Single-cell, real-time detection of oxidative stress induced in *Escherichia coli* by the antimicrobial peptide CM15. *Proceedings of the National Academy of Sciences of the United States of America, 112*(3), E303-E310. doi:doi:10.1073/pnas.1417703112.

Collins, B., Curtis, N., Cotter, P. D., Hill, C., & Ross, R. P. (2010a). The ABC transporter AnrAB contributes to the innate resistance of *Listeria monocytogenes* to nisin, bacitracin, and various beta-lactam antibiotics. *Antimicrobial Agents and Chemotherapy, 54*(10), 4416–4423.

Collins, B., Guinane, C. M., Cotter, P. D., Hill, C., & Ross, R. P. (2012). Assessing the contributions of the LiaS histidine kinase to the innate resistance of *Listeria monocytogenes* to nisin, cephalosporins, and disinfectants. *Applied and Environmental Microbiology, 78*(8), 2923–2929. https://doi.org/10.1128/AEM.07402-11

Collins, B., Joyce, S., Hill, C., Cotter, P. D., & Ross, R. P. (2010b). TelA contributes to the innate resistance of *Listeria monocytogenes* to nisin and other cell wall-acting antibiotics. *Antimicrobial Agents and Chemotherapy, 54*(11), 4658–4663. https://doi.org/10.1128/AAC.00290-10

Consortium, T. U. (2022). UniProt: the universal protein knowledgebase in 2023. *Nucleic Acids Res, 51*(D1), D523-D531. doi:10.1093/nar/gkac1052.

Cox, J., & Mann, M. (2008). MaxQuant enables high peptide identification rates, individualized p.p.b.-range mass accuracies and proteome-wide protein quantification. *Nature Biotechnology, 26*(12), 1367–1372. https://doi.org/10.1038/nbt.1511

Delmar, J. A., Su, C.-C., & Yu, E. W. (2014). Bacterial multidrug efflux transporters. *Annual Review of Biophysics, 43*(1), 93–117. https://doi.org/10.1146/annurev-biophys-051013-022855

Domínguez-Escobar, J., Wolf, D., Fritz, G., Höfler, C., Wedlich-Söldner, R., & Mascher, T. (2014). Subcellular localization, interactions and dynamics of the phage-shock protein-like Lia response in *Bacillus subtilis*. *Molecular Microbiology, 92*(4), 716–732. https://doi.org/10.1111/mmi.12586

EFSA and ECDC (European Food Safety Authority and European Centre for Disease Prevention and Control). (2022). The European Union One Health 2021 Zoonoses Report. *EFSA Journal, 20*(12), 273. https://doi.org/10.2903/j.efsa.2022.7666

Feng, Y., Bui, T. P. N., Stams, A. J. M., Boeren, S., Sánchez-Andrea, I., & de Vos, W. M. (2022). Comparative genomics and proteomics of *Eubacterium maltosivorans*: Functional identification of trimethylamine methyltransferases and bacterial microcompartments in a human intestinal bacterium with a versatile lifestyle. *Environmental Microbiology, 24*(1), 517–534. https://doi.org/10.1111/1462-2920.15886

Flores-Kim, J., & Darwin, A. J. (2016). The phage shock protein response. *Annual Review of Microbiology, 70*, 83–101. https://doi.org/10.1146/annurev-micro-102215-095359

Forauer, E., Wu, S. T., & Etter, A. J. (2021). *Listeria monocytogenes* in the retail deli environment: A review. *Food Control, 119*. https://doi.org/10.1016/j.foodcont.2020.107443

Fritsch, F., Mauder, N., Williams, T., Weiser, J., Oberle, M., & Beier, D. (2011). The cell envelope stress response mediated by the LiaFSRLm three-component system of *Listeria monocytogenes* is controlled via the phosphatase activity of the bifunctional histidine kinase LiaSLm. *Microbiol, 157*(2), 373–386. https://doi.org/10.1099/mic.0.044776-0

Gandhi, M., & Chikindas, M. L. (2007). *Listeria*: A foodborne pathogen that knows how to survive. *International Journal of Food Microbiology, 113*(1), 1–15. https://doi.org/10.1016/j.ijfoodmicro.2006.07.008

Gangwar, B., Kumar, S., & Darokar, M. P. (2020). Glabridin averts biofilms formation in methicillin-resistant *Staphylococcus aureus* by modulation of the surfaceome. *Frontiers in Microbiology, 11*, 1779. https://doi.org/10.3389/fmicb.2020.01779

Greene, N. P., Kaplan, E., Crow, A., & Koronakis, V. (2018). Antibiotic resistance mediated by the MacB ABC transporter family: A structural and functional perspective. *Frontiers in Microbiology, 9*. https://doi.org/10.3389/fmicb.2018.00950

Guariglia-Oropeza, V., Orsi, R. H., Guldimann, C., Wiedmann, M., & Boor, K. J. (2018). The *Listeria monocytogenes* bile stimulon under acidic conditions is characterized by strain-specific patterns and the upregulation of motility, cell wall modification

functions, and the PrfA regulon. *Frontiers in Microbiology, 9*. https://doi.org/10.3389/fmicb.2018.00120
Guerreiro, D. N., Arcari, T., & O'Byrne, C. P. (2020). The sigma(B)-mediated general stress response of Listeria monocytogenes: Life and death decision making in a pathogen. *Frontiers in Microbiology, 11*, 1505. https://doi.org/10.3389/fmicb.2020.01505
Hain, T., Hossain, H., Chatterjee, S. S., Machata, S., Volk, U., Wagner, S., … Chakraborty, T. (2008). Temporal transcriptomic analysis of the *Listeria monocytogenes* EGD-e sigmaB regulon. *BMC Microbiology, 8*, 20. https://doi.org/10.1186/1471-2180-8-20
Illigmann, A., Thoma, Y., Pan, S., Reinhardt, L., & Brötz-Oesterhelt, H. (2021). Contribution of the Clp protease to bacterial survival and mitochondrial homoeostasis. *Microb Physiol, 31*(3), 260–279. https://doi.org/10.1159/000517718
Jiang, X., Geng, Y., Ren, S., Yu, T., Li, Y., Liu, G., … Shi, L. (2019). The VirAB-VirSR-AnrAB multicomponent system is involved in resistance of *Listeria monocytogenes* EGD-e to cephalosporins, bacitracin, nisin, benzalkonium chloride, and ethidium bromide. *Applied and Environmental Microbiology, 85*(20), e01470–e11419. https://doi.org/10.1128/AEM.01470-19
Joly, N., Engl, C., Jovanovic, G., Huvet, M., Toni, T., Sheng, X., … Buck, M. (2010). Managing membrane stress: The phage shock protein (Psp) response, from molecular mechanisms to physiology. *FEMS Microbiology Reviews, 34*(5), 797–827. https://doi.org/10.1111/j.1574-6976.2010.00240.x
Jordan, S., Hutchings, M. I., & Mascher, T. (2008). Cell envelope stress response in Gram-positive bacteria. *FEMS Microbiology Reviews, 32*(1), 107–146. https://doi.org/10.1111/j.1574-6976.2007.00091.x
Kalli, S., Araya-Cloutier, C., Hageman, J., & Vincken, J. P. (2021). Insights into the molecular properties underlying antibacterial activity of prenylated (iso)flavonoids against MRSA. *Scientific Reports, 11*(1), 14180. https://doi.org/10.1038/s41598-021-92964-9
Kang, J., Wiedmann, M., Boor, K. J., & Bergholz, T. M. (2015). VirR-Mediated resistance of *Listeria monocytogenes* against food antimicrobials and cross-protection induced by exposure to organic acid salts. *Applied and Environmental Microbiology, 81*(13), 4553–4562. https://doi.org/10.1128/AEM.00648-15
Karatzas, K. A., Suur, L., & O'Byrne, C. P. (2012). Characterization of the intracellular glutamate decarboxylase system: Analysis of its function, transcription, and role in the acid resistance of various strains of *Listeria monocytogenes*. *Applied and Environmental Microbiology, 78*(10), 3571–3579. https://doi.org/10.1128/AEM.00227-12
Kazmierczak, M. J., Mithoe, S. C., Boor, K. J., & Wiedmann, M. (2003). *Listeria monocytogenes* sigma B regulates stress response and virulence functions. *Journal of Bacteriology, 185*(19), 5722–5734. https://doi.org/10.1128/jb.185.19.5722-5734.2003
Koomen, J., Huijboom, L., Ma, X., Tempelaars, M. H., Boeren, S., Zwietering, M. H., … Abee, T. (2021). Amino acid substitutions in ribosomal protein RpsU enable switching between high fitness and multiple-stress resistance in *Listeria monocytogenes*. *International Journal of Food Microbiology, 351*, Article 109269. https://doi.org/10.1016/j.ijfoodmicro.2021.109269
Laursen, M. F., Bahl, M. I., Licht, T. R., Gram, L., & Knudsen, G. M. (2015). A single exposure to a sublethal pediocin concentration initiates a resistance-associated temporal cell envelope and general stress response in *Listeria monocytogenes*. *Environmental Microbiology, 17*(4), 1134–1151. https://doi.org/10.1111/1462-2920.12534
Lin, H., Hu, J., Mei, F., Zhang, Y., Ma, Y., Chen, Q., … Yang, Y. (2022). Anti-microbial efficacy, mechanisms and druggability evaluation of the natural flavonoids. *Journal of Applied Microbiology, 133*(3), 1975–1988. https://doi.org/10.1111/jam.15705
Liu, F., Liu, M., Du, L., Wang, D., Geng, Z., Zhang, M., … Xu, W. (2015). Synergistic antibacterial effect of the combination of ε-polylysine and nisin against *Enterococcus faecalis*. *Journal of Food Protection, 78*(12), 2200–2206. https://doi.org/10.4315/0362-028x.Jfp-15-220
Liu, Y., Orsi, R. H., Boor, K. J., Wiedmann, M., & Guariglia-Oropeza, V. (2017). Home alone: Elimination of all but one alternative sigma factor in Listeria monocytogenes allows prediction of new roles for sigma(B). *Frontiers in Microbiology, 8*, 1910. https://doi.org/10.3389/fmicb.2017.01910
Liu, Y., Tempelaars, M. H., Boeren, S., Alexeeva, S., Smid, E. J., & Abee, T. (2022). Extracellular vesicle formation in *Lactococcus lactis* is stimulated by prophage-encoded holin-lysin system. *Microbial Biotechnology, 15*(4), 1281–1295. https://doi.org/10.1111/1751-7915.13972
Mandin, P., Fsihi, H., Dussurget, O., Vergassola, M., Milohanic, E., Toledo-Arana, A., … Cossart, P. (2005). VirR, a response regulator critical for *Listeria monocytogenes* virulence. *Molecular Microbiology, 57*(5), 1367–1380. https://doi.org/10.1111/j.1365-2958.2005.04776.x
Mascher, T., Margulis, N. G., Wang, T., Ye, R. W., & Helmann, J. D. (2003). Cell wall stress responses in *Bacillus subtilis*: The regulatory network of the bacitracin stimulon. *Molecular Microbiology, 50*(5), 1591–1604. https://doi.org/10.1046/j.1365-2958.2003.03786.x
Mattila, M., Somervuo, P., Korkeala, H., Stephan, R., & Tasara, T. (2020). Transcriptomic and phenotypic analyses of the sigma b-dependent characteristics and the synergism between sigma B and sigma L in *Listeria monocytogenes* EGD-e. *Microorganisms, 8*(11). https://doi.org/10.3390/microorganisms8111644
Miyamoto, K. N., Monteiro, K. M., da Silva Caumo, K., Lorenzatto, K. R., Ferreira, H. B., & Brandelli, A. (2015). Comparative proteomic analysis of *Listeria monocytogenes* ATCC 7644 exposed to a sublethal concentration of nisin. *Journal of Proteomics, 119*, 230–237. https://doi.org/10.1016/j.jprot.2015.02.006
Ng, K. R., Lyu, X., Mark, R., & Chen, W. N. (2019). Antimicrobial and antioxidant activities of phenolic metabolites from flavonoid-producing yeast: Potential as natural food preservatives. *Food Chemistry, 270*, 123–129. https://doi.org/10.1016/j.foodchem.2018.07.077
NicAogain, K., & O'Byrne, C. P. (2016). The role of stress and stress adaptations in determining the fate of the bacterial pathogen *Listeria monocytogenes* in the food chain. *Frontiers in Microbiology, 7*, 1865. https://doi.org/10.3389/fmicb.2016.01865
Nielsen, P. K., Andersen, A. Z., Mols, M., van der Veen, S., Abee, T., & Kallipolitis, B. H. (2012). Genome-wide transcriptional profiling of the cell envelope stress response and the role of LisRK and CesRK in *Listeria monocytogenes*. *Microbiology, 158*(4), 963–974. https://doi.org/10.1099/mic.0.055467-0
Oliveira, A. R., Domingues, F. C., & Ferreira, S. (2017). The influence of resveratrol adaptation on resistance to antibiotics, benzalkonium chloride, heat and acid stresses of *Staphylococcus aureus* and *Listeria monocytogenes*. *Food Control, 73*, 1420–1425. https://doi.org/10.1016/j.foodcont.2016.11.011
Oliver, H. F., Orsi, R. H., Wiedmann, M., & Boor, K. J. (2010). *Listeria monocytogenes* σB has a small core regulon and a conserved role in virulence but makes differential contributions to stress tolerance across a diverse collection of strains. *Applied and Environmental Microbiology, 76*(13), 4216–4232. https://doi.org/10.1128/aem.00031-10
Ollinger, J., Bowen, B., Wiedmann, M., Boor, K. J., & Bergholz, T. M. (2009). *Listeria monocytogenes* sigmaB modulates PrfA-mediated virulence factor expression. *Infection and Immunity, 77*(5), 2113–2124. https://doi.org/10.1128/iai.01205-08
Pang, D., Liao, S., Wang, W., Mu, L., Li, E., Shen, W., … Zou, Y. (2019). Destruction of the cell membrane and inhibition of cell phosphatidic acid biosynthesis in *Staphylococcus aureus*: An explanation for the antibacterial mechanism of morusin. *Food & Function, 10*(10), 6438–6446. https://doi.org/10.1039/c9fo01233h
Pang, X., Wu, Y., Liu, X., Wu, Y., Shu, Q., Niu, J., … Zhang, X. (2022). the lipoteichoic acid-related proteins YqgS and LafA contribute to the resistance of *Listeria monocytogenes* to nisin. *Microbiol Spectr, 10*(1), e02095–e12021. https://doi.org/10.1128/spectrum.02095-21
Pinilla, C. M. B., Stincone, P., & Brandelli, A. (2021). Proteomic analysis reveals differential responses of *Listeria monocytogenes* to free and nanoencapsulated nisin. *International Journal of Food Microbiology, 346*, Article 109170. https://doi.org/10.1016/j.ijfoodmicro.2021.109170
Po, K. H. L., Chow, H. Y., Cheng, Q., Chan, B.-K.-W., Deng, X., Wang, S., … Chen, S. (2021). Daptomycin exerts bactericidal effect through induction of excessive ROS production and blocking the function of stress response protein Usp2. *Natural Science, 1*(2), e10023.
Popp, P. F., Gumerov, V. M., Andrianova, E. P., Bewersdorf, L., Mascher, T., Zhulin, I. B., & Wolf, D. (2022). Phyletic distribution and diversification of the phage shock protein stress response system in bacteria and archaea. *mSystems, 7*(3), e01348–e11321. https://doi.org/10.1128/msystems.01348-21
R Core Team. (2020). *R: A language and environment for statistical computing*. Vienna, Austria: R Foundation for Statistical Computing. https://www.R-project.org/.
Rismondo, J., & Schulz, L. M. (2021). Not just transporters: Alternative functions of abc transporters in *Bacillus subtilis* and *Listeria monocytogenes*. *Microorganisms, 9*(1), 163. https://www.mdpi.com/2076-2607/9/1/163.
Ryan, S., Begley, M., Gahan, C. G., & Hill, C. (2009). Molecular characterization of the arginine deiminase system in *Listeria monocytogenes*: Regulation and role in acid tolerance. *Environmental Microbiology, 11*(2), 432–445. https://doi.org/10.1111/j.1462-2920.2008.01782.x
Schäfer, A.-B., & Wenzel, M. (2020). A how-to guide for mode of action analysis of antimicrobial peptides. *Frontiers in Cellular and Infection Microbiology, 10*. https://doi.org/10.3389/fcimb.2020.540898
Singh, V., Pal, A., & Darokar, M. P. (2015). A polyphenolic flavonoid glabridin: Oxidative stress response in multidrug-resistant *Staphylococcus aureus*. *Free Radical Biology & Medicine, 87*, 48–57. https://doi.org/10.1016/j.freeradbiomed.2015.06.016
Sivaranjani, M., Leskinen, K., Aravindraja, C., Saavalainen, P., Pandian, S. K., Skurnik, M., & Ravi, A. V. (2019). Deciphering the antibacterial mode of action of alpha-mangostin on *Staphylococcus epidermidis* RP62A through an integrated transcriptomic and proteomic approach. *Frontiers in Microbiology, 10*, 150. https://doi.org/10.3389/fmicb.2019.00150
Song, M., Liu, Y., Li, T., Liu, X., Hao, Z., Ding, S., … Shen, J. (2021). Plant natural flavonoids against multidrug resistant pathogens. *Adv Sci (Weinh), 8*(15), e2100749.
Soni, K. A., Nannapaneni, R., & Tasara, T. (2011). The contribution of transcriptomic and proteomic analysis in elucidating stress adaptation responses of *Listeria monocytogenes*. *Foodborne Pathogens and Disease, 8*(8), 843–852. https://doi.org/10.1089/fpd.2010.0746
Steinfels, E., Orelle, C., Fantino, J.-R., Dalmas, O., Rigaud, J.-L., Denizot, F., … Jault, J.-M. (2004). Characterization of YvcC (BmrA), a multidrug ABC transporter constitutively expressed in Bacillus subtilis. *Biochemistry, 43*(23), 7491–7502. https://doi.org/10.1021/bi0362018
Toledo-Arana, A., Dussurget, O., Nikitas, G., Sesto, N., Guet-Revillet, H., Balestrino, D., … Cossart, P. (2009). The *Listeria* transcriptional landscape from saprophytism to virulence. *Nature, 459*(7249), 950–956. https://doi.org/10.1038/nature08080
Tsukatani, T., Kuroda, R., & Kawaguchi, T. (2022). Screening biofilm eradication activity of ethanol extracts from foodstuffs: Potent biofilm eradication activity of glabridin, a major flavonoid from licorice (Glycyrrhiza glabra), alone and in combination with ε-poly-l-lysine. *World Journal of Microbiology and Biotechnology, 38*(2), 24. https://doi.org/10.1007/s11274-021-03206-z
Tyanova, S., Temu, T., Sinitcyn, P., Carlson, A., Hein, M. Y., Geiger, T., … Cox, J. (2016). The Perseus computational platform for comprehensive analysis of (prote)omics data. *Nature Methods, 13*(9), 731–740. https://doi.org/10.1038/nmeth.3901
van Dinteren, S., Meijerink, J., Witkamp, R., van Ieperen, B., Vincken, J. P., & Araya-Cloutier, C. (2022). Valorisation of liquorice (*Glycyrrhiza*) roots: antimicrobial activity and cytotoxicity of prenylated (iso)flavonoids and chalcones from liquorice spent (*G. glabra, G. inflata, and G. uralensis*). *Food Funct*. doi:10.1039/d2fo02197h.

Vizcaíno, J. A., Csordas, A., del-Toro, N., Dianes, J. A., Griss, J., Lavidas, I., Mayer, G., Perez-Riverol, Y., Reisinger, F., Ternent, T., Xu, Q. W., Wang, R., & Hermjakob, H. (2016). 2016 update of the PRIDE database and its related tools. *Nucleic Acids Res, 44* (D1), D447-456. doi:10.1093/nar/gkv1145.

Wemekamp-Kamphuis, H. H., Wouters, J. A., de Leeuw, P. P., Hain, T., Chakraborty, T., & Abee, T. (2004). Identification of sigma factor sigma B-controlled genes and their impact on acid stress, high hydrostatic pressure, and freeze survival in *Listeria monocytogenes* EGD-e. *Applied and Environmental Microbiology, 70*(6), 3457–3466. https://doi.org/10.1128/aem.70.6.3457-3466.2004

Wesolowska, O., Gasiorowska, J., Petrus, J., Czarnik-Matusewicz, B., & Michalak, K. (2014). Interaction of prenylated chalcones and flavanones from common hop with phosphatidylcholine model membranes. *Biochim Biophys Acta, 1838*(1 Pt B), 173-184. doi:10.1016/j.bbamem.2013.09.009.

Wisniewski, J. R., Zougman, A., Nagaraj, N., & Mann, M. (2009). Universal sample preparation method for proteome analysis. *Nature Methods, 6*(5), 359–362. https://doi.org/10.1038/nmeth.1322

Wu, S. C., Han, F., Song, M. R., Chen, S., Li, Q., Zhang, Q., … Shen, J. Z. (2019a). Natural flavones from morus alba against methicillin-resistant *Staphylococcus aureus* via targeting the proton motive force and membrane permeability. *Journal of Agricultural and Food Chemistry, 67*(36), 10222–10234. https://doi.org/10.1021/acs.jafc.9b01795

Wu, S. C., Yang, Z. Q., Liu, F., Peng, W. J., Qu, S. Q., Li, Q., … Shen, J. Z. (2019b). Antibacterial effect and mode of action of flavonoids from licorice against methicillin-resistant *Staphylococcus aureus*. *Frontiers in Microbiology, 10*, 2489. https://doi.org/10.3389/fmicb.2019.02489

Yang, S. K., Tan, N. P., Chong, C. W., Abushelaibi, A., Lim, S. H., & Lai, K. S. (2021). The missing piece: recent approaches investigating the antimicrobial mode of action of essential oils. *Evol Bioinform Online, 17*, 1176934320938391. doi:10.1177/1176934320938391.

Zhang, H., Yamamoto, E., Murphy, J., & Locas, A. (2020). Microbiological safety of ready-to-eat fresh-cut fruits and vegetables sold on the Canadian retail market. *International Journal of Food Microbiology, 335*, Article 108855. https://doi.org/10.1016/j.ijfoodmicro.2020.108855